BURIAL RATE DETERMINES HOLOCENE RHODOLITH DEVELOPMENT ON THE BRAZILIAN SHELF

POLIANA S. BRASILEIRO,[1] JUAN C. BRAGA,[2] GILBERTO M. AMADO-FILHO,[1] RACHEL N. LEAL,[1] DAVIDE BASSI,[3] TARCILA FRANCO,[4] ALEX C. BASTOS,[4] AND RODRIGO L. MOURA[5]

[1]Instituto de Pesquisas Jardim Botanicoˆ do Rio de Janeiro, Rua Pacheco Leaˇo 915, 22460-030 Rio de Janeiro, RJ, Brazil
[2]Departamento de Estratigrafˊıa y Paleontologˊıa, Universidad de Granada, Campus Fuentenueva, s/n, 18002, Granada, Spain
[3]Dipartimento di Fisica e Scienze della Terra, Universita` degli Studi di Ferrara, via Saragat 1, I-44122 Ferrara, Italy
[4]Departamento de Oceanografia, Universidade Federal do Espˊırito Santo, Avenida Fernando Ferrari 514, 29090-600 Vitoria,ˊ ES, Brazil
[5]Departamento de Biologia Marinha, Instituto de Biologia, Universidade Federal do Rio de Janeiro, CP68011, 21944-970, Rio de Janeiro, RJ, Brazil email: gfilho@jbrj.gov.br

ABSTRACT: The structure and composition of rhodoliths in two regions of the Brazilian shelf, Abrolhos Continental Shelf (ACS) and South Espˊırito Santo State (SES) were examined and compared. Rhodoliths were sampled at depth ranges of 10–20 m and 50–60 m in SES, and 20–30 m and 50–75 m in ACS. Rhodoliths in SES are algal boundstones, built mainly of melobesioid corallines, with subordinate bryozoans and encrusting foraminifers. They show high porosity and the sediment infill of borings and voids contains a relatively high amount of siliciclastics (up to 8%). Rhodoliths from ACS are formed by a structureless carbonate mass covered by a thin veneer of encrusting coralline algae. The massive interior was produced by multiphase boring and infilling of an original boundstone. The infillings consist of a micritic matrix with bioclasts and low amounts of siliciclastic grains. Coralline assemblages are reduced to fragments of thin crusts. Rhodoliths from shallow depths are small (, 8 cm) whereas rhodoliths from the deeper zone have a wide size range (1 to 17 cm). The innermost parts of deeper rhodoliths in ACS yield radiocarbon ages of ~ 7,000 years BP (75 m) and ~ 2,000 years BP (65 m). Rhodoliths from the deep zone in SES are younger (less than 700 years BP). Siliciclastic sediment influx reaching rhodolith beds promotes burial of rhodoliths, determining the small size of shallow SES rhodoliths and the relatively young ages of the deeper ones. Scarce siliciclastic influx at the ACS rhodolith beds favors long residence times of rhodoliths on the seafloor, resulting in a thorough destruction of the original coralline/invertebrate boundstone by bioerosion.

INTRODUCTION

Rhodoliths are free-living calcareous nodules, formed primarily by coralline red algae (50%), with other organisms, such as bryozoans and serpulids, as secondary components (Foster 2001). Rhodoliths can occur in large concentrations on the sea floor, known as rhodolith beds, which occur worldwide in a wide depth range on marine shelves (Foster 2001; Kamenos et al. 2017).

The Brazilian continental shelf encompasses the largest nearly continuous rhodolith beds in the world (Amado-Filho et al. 2012a). These beds, however, are not uniform since they differ in the rhodolith-forming species of crustose coralline algae, associated macroalgal assemblages, and density of nodules, which vary in size from less than one to tens of centimeters (Testa and Bosence 1999; Amado-Filho et al. 2010, 2012a, 2012b, 2016; Pereira-Filho et al. 2012; Pascelli et al. 2013; Brasileiro et al. 2015). In total, 33 rhodolith-forming species of coralline algae have been reported in the Brazilian shelf (Amado-Filho et al. 2017).

Despite the increasing knowledge about Brazilian rhodoliths in the last decade, little is known about their inner arrangement and composition (Leal et al. 2012; Tamega et al. 2014; Vale et al. 2018). The taxonomic composition, morphology, inner structure, and interactions of coralline algae with other encrusting groups (such as bryozoans, corals, and serpulids) are relevant for understanding the factors that control long-term development of rhodoliths (Adey and MacIntyre 1973; Aguirre et al. 2012) and to reconstruct the paleoenvironments in which they grew (Bosence 1983a; Braga and Aguirre 2001; Bassi et al. 2009; Braga et al. 2010; Brandano et al. 2010; Aguirre et al. 2012, 2017). Significant features of the inner arrangement of rhodoliths include the nature of the nucleus, constructional spaces and their sediment infilling, and succession of growth-forms of the rhodolith-forming organisms from the inner to the outer layers. The presence and density of bioerosion also determines the inner structure of rhodoliths (Bassi et al. 2012, 2013; Aguirre et al. 2017). The biological activity of bioeroders can deeply influence the development and preservation of rhodolith structure, and consequently the potential of rhodoliths for paleoenvironmental reconstruction (Nebelsick and Bassi 2000; Aguirre et al. 2017).

Here, we analyze with an actuopaleontological approach the morphol-ogy, taxonomic composition and inner structure of rhodoliths from the sea floor in two regions of the Brazilian coast, Abrolhos Continental Shelf (ACS) and South Espˊırito Santo State (SES). Within each region rhodoliths were collected at two different depth ranges. These two areas represent distinct domains of the Brazilian coast, especially distinguished by the width of the shelf (~ 50 km at SES and ~ 200 km at ACS), and therefore the proximity to the shoreline. These characteristics are closely related to sediment type and distribution, availability of nutrients, and water turbidity, which can influence the development, structure, and composition of rhodoliths. The aims of this study are: (1) to understand the factors controlling the long-term development of the coralline nodules in areas in which they are major ecosystem engineers (sensu Jones et al. 1997); and

to provide patterns of rhodolith morphology, taxonomic composition, and internal structure throughout environmental gradients, which could be applied to reconstruct paleoenvironments of formation of fossil rhodolith beds, common in Cenozoic and Quaternary shallow-water marine deposits. The contrasting internal arrangement of rhodoliths from two regions (SES and ACS) with similar productivity and water surface temperatures suggests that burial rate is a major factor controlling the long term structure of coralline algal nodules. Delayed burial in ACS rhodoliths due to low sediment influx favors long-lasting bioerosion, which obliterates the original coralline algal/invertebrate framework.

ENVIRONMENTAL SETTING OF STUDY AREAS

SES and ACS (Fig. 1) are located along the eastern Brazilian continental shelf. The Espirito Santo shelf is narrow, ranging from 30 to 60 km in width, whereas the Abrolhos shelf reaches up to 200 km in width. Sediment distribution shows distinct domains that vary along and across-shelf. Rhodolith beds predominate over the entire outer shelf, coral reefs occur along the northern Abrolhos inner shelf, and terrigenous mud deposits are associated to the Doce River on the adjacent shelf. The narrow SES shelf is characterized by mixed siliciclastic-carbonate sedimentation in the inner shelf and rhodolith beds along mid- and outer-shelf (Bastos et al. 2015) (Fig. 1).

The Doce River is the main sediment source for the area, with an annual average discharge of 700 m^3/s and sediment load of 60310^6 tons (Oliveira and Quaresma 2017). In ACS, sea surface temperature ranges from 22 to 298C and chlorophyll a annual values range from 0.17 to 1.6 lg/l (Bruce et al. 2012; Ghisolfi et al. 2015). SES is influenced by coastal upwelling during the summer months. Sea surface temperatures range from 24 to 288C, but during deep-water intrusion, bottom temperature can descend to 16.58C on the shelf (Paloczy et al. 2016). Chlorophyll a measured during two years in an area situated 40 km north of studied sites at SES ranges from 0.11 to 1.55 lg/l (average 0.47 lg/l) (Costa et al. 2014).

MATERIAL AND METHODS

The present work is an actuopaleontological study of rhodolith samples from living rhodolith beds from SES (Figs. 1, 2), which were described by Amado-Filho et al. (2007, 2010), and Marins et al. (2014), and from ACS (Figs. 1, 2), analyzed by Amado-Filho et al. (2012a) and Brasileiro et al. (2015). A complete description of the variety of ecosystems of the entire ACS can be found in Moura et al. (2013).

Rhodoliths from SES were collected by scuba diving at two depth ranges, where rhodolith beds occur, 10–20 m (sites E1 and E2) and 50–60 m (site E3), between 3 and 45 km offshore, in November 2005 (Table 1, Fig. 1). In total, 100 rhodoliths were collected. Rhodoliths from ACS were collected by scuba and technical diving at 20–30 m (sites A1 and A2) and 50–75 m (sites A3 and A4), in October 2009 (Table 1, Fig. 1). As there are no rhodolith beds shallower than 20 m on the central ACS, these two depth ranges were selected as the closest to compare with the previously sampled depth ranges of rhodolith beds in SES. In total 405 rhodolith samples were collected in the central region of ACS, in its largest extension, between 100 and 150 km offshore (Fig. 1).

Size and shape were determined by measuring the longest, intermediate, and shortest axes of each nodule, following Sneed and Folk (1958) in all collected rhodoliths (100 from SES and 405 from ACS).

To estimate the percentage of calcium carbonate, organic matter, and siliciclastic grains, five rhodoliths were randomly taken from each region and depth range (total 20 rhodoliths) and cut along their longest axis. About 5 g of powder were randomly extracted with a microdrill from several locations on the cut surface. The powder was weighed and exposed to hydrochloric acid (HCl, 30%) in excess until the calcium carbonate was

TABLE 1.—Regions, sample sites, latitude-longitude, depths and collecting dates of studied samples.

Region	Sample site	Latitude (S)	Longitude (W)	Depth (m)	Date
SES	E1	20855^0 27^{00}	40845^0 22^{00}	10–20	November 2005
SES	E2	21801^0 57^{00}	40840^0 54^{00}	10–20	November 2005
SES	E3	21802^0 58^{00}	40817^0 49^{00}	50–60	November 2005
ACS	A1	17853^0 55^{00}	38818^0 34^{00}	20–30	October 2009
ACS	A2	17848^0 35^{00}	38811^0 03^{00}	20–30	October 2009
ACS	A3	17854^0 03^{00}	38812^0 39^{00}	50–60	October 2009
ACS	A4	17854^0 01^{00}	37854^0 59^{00}	50–75	October 2009

dissolved (the mixture stopped forming bubbles). The samples were then washed, oven dried, and weighed again to determine the lost carbonate content. The organic matter was then removed with hydrogen peroxide (H_2O_2, 30%) and the sample weighed again to determine the siliciclastic content.

To study their inner arrangement and composition, 40 rhodoliths (10 from each depth zone in both areas) were cut along their longest axis and their halves were photographed (camera Nikon D90). Eight thin sections were made from the cut surface of rhodoliths from shallow SES, 10 from the deep SES, 12 from shallow and 11 from deep ACS, in the National Petrographic Service, Inc. (Houston, Texas, USA). In large rhodoliths two successive thin sections were cut from the center to the outer surface. Thin sections were examined under an Olympus BX43 optical microscope with digital camera (Moticam) attached. Images were captured using the Dynamic Scope Image Pro 2009 software. Fossil components were identified to the most precise taxonomic level possible based on the literature. Specifically, coralline algae were identified following the available accounts of living corallines in the Brazilian Shelf (Bahia et al. 2010; Bahia 2014; Brasileiro et al. 2015). The relative abundance of the organisms building the rhodoliths, trace fossils, and empty spaces (with and without filling) was estimated by point counting on images made from the thin sections (consistently at the same scale). A total of ~ 300 points were determined per thin section using the image-analysis software Coral Count Point with Excel extensions (CPCe v 4.1). A non-metric multidimensional scaling (MDS) based on the data compiled was performed to rank the similarity of samples analyzed. The similarity matrix used in MDS was based on the Bray-Curtis index and abundance values were calculated using a fourth-root transformation (Clarke and Warwick 1994). Multivariate analyses were performed using the program Primer v. 6.0.

Five subsamples of rhodoliths (two from deep SES and three from ACS) were selectively drilled for radiocarbon dating. Microdrilling targeted CCA visible at the cut surface along the major axis of rhodoliths. Four samples were also obtained from the structureless mass (see below) of three ACS rhodoliths due to the lack of CCA large enough to be selectively drilled. Powder samples were analyzed in the Center of Applied Isotope Studies (University of Georgia, Georgia, USA) with Accelerator Mass Spectrom-etry (AMS). Results were derived from reduction of sample carbon after acid-etch pretreatment to graphite (100% C) with subsequent detection in AMS. The dates are reported as calendar years BP (‘‘present’’ ¼ AD 1950) using the 2 d confidence interval as median calibrated years.

RESULTS

No differences in structure and composition were observed between rhodoliths from sampling sites within the same depth range (hereafter termed zone) in any of the regions. By contrast, rhodoliths from different zones (Fig. 2) show marked dissimilarity in several features of their internal structure and composition. The main characteristics of rhodoliths from each region and zones are described in the following sections.

Shallow South Esp´ırito Santo (10–20 m)

Rhodoliths from SES shallow zone have the smallest mean diameter (4.7 6 1.2 cm) (Figs. 2, 3, Table 2) and no large rhodoliths (size classes . 8 cm) were found. Most rhodoliths are spheroidal to subspheroidal (Fig. 4), with an asymmetric concentric to boxwork inner arrangement. They consist of encrusting (Figs. 5A, 6A, 6B) to warty (Fig. 5B), lumpy, and fruticose (Fig. 5E) coralline algae (~ 54%), growing one upon the other and intergrown with other encrusters, mainly bryozoans (~ 11%) (Fig. 6A, Table 5). Coral fragments often form the nucleus (Figs. 5C, 5E, 6B). Lithothamnion crispatum is the most frequent coralline alga both at the surface and rhodolith interior (Fig. 6A, 6B); Melyvonnea erubescens, Spongites sp., Sporolithon sp., and Lithophyllum sp. also occur (Table 6). In addition to framework voids created by encrusting organisms, empty spaces caused by the dissolution of aragonite skeletons are frequent (Fig. 5C). Borings and voids are filled by two phases of grainstone to wackestone (Fig. 6A, 6B). Microborings can be observed in coralline algae and corals. Siliciclastic grains and organic matter account for 5.4% and 4.6% of the rhodoliths, respectively (Table 4).

Deep South Esp´ırito Santo (50–60 m)

Rhodoliths from the deeper SES zone show the largest mean diameter (8.7 6 2.2 cm), with few representatives of the smallest size classes (0–2 and 2–4 cm) (Figs. 2, 3, Table 2). Most rhodoliths are spheroidal to subspheroidal with lesser amounts of ellipsoidal and discoidal nodules (Fig. 4). They have a boxwork inner organization, made of encrusting and foliose coralline algae (~ 35%), and bryozoans (~ 20%) associated with foraminifers (Figs. 5F–5I, 6C–6E, Table 5). Lithothamnion crispatum is the dominant living coralline at rhodolith surfaces, with minor Sporolithon and Lithophyllum plants. Lithothamnion crispatum (Fig. 6D), Lithothamnion muelleri (Fig. 6E), Sporolithon sp., Lithophyllum species, and unidentifiable melobesioids are the recognizable corallines (Table 6) inside rhodoliths. Constructional voids account for more than 12% of the volume (Fig. 6D, 6E, Table 5). Borings and voids are filled by three to four phases of sediment consisting of wackestone to packstone with mixed siliciclastic grains (Fig. 6C–6E, Table 3), more abundant in the third and fourth phases. Rhodoliths show the lowest percentage of calcium carbonate in the study zones (7.9% of siliciclastics, and 4.1% of organic matter, on average; Table 4). The boring fillings are rich in ascidian and sponge spicules; articulated coralline algae and foraminifers are frequent, whereas bivalve and echinoderm fragments are rare. No corals were recorded at this depth. Microborings are common in coralline algal thalli.

Shallow Abrolhos Continental Shelf (20–30 m)

Rhodoliths from the ACS shallow zone have a wide size range, from ~ 1 to ~ 17 cm, with a mean diameter close to 7 cm (Fig. 3, Table 2). They are mostly spheroidal to subspheroidal (~ 89 %, see Fig. 4, Table 2), with asymmetric inner arrangement (Fig. 7A–7D). The rhodoliths were probably originally formed by encrusting corallines, intergrown with invertebrates (including corals) and foraminifers, but all the specimens examined consist of a thin veneer of encrusting corallines partially or totally covering a structureless carbonate mass consisting of borings with partial wackestone to packstone infills (Fig. 8A, 8B). At rhodolith scale, this mass is the ‘‘end member’’ of destruction of an algal framework by multiple phases of boring and infilling. Similar destructive multistory bioerosion can be observed in the ‘‘reef rock’’ of coralline algal reefs in Bermuda (Ginsburg and Schroeder 1973) and the framework of algal reefs in St. Croix (Caribbean, Bosence 1983b, 1984), although in these two cases the structure of coralline frameworks is still preserved. The structureless mass is the result of at least three to four phases of bioperforation and three phases of filling by a carbonate matrix rich in ascidian and sponge spicules (Fig. 8C), articulated coralline algae, foraminifers, and coral as well as bivalve fragments. Bioclasts of Halimeda, echinoderms and brachiopods are rare. Bioerosion destroyed the original coralline/invertebrate/foramineral rhodolith framework and successive infillings of borings and voids were also affected by later bioperforation. Rhodoliths from this depth contain an average of 2.7% of siliciclastics and 1.6% of organic matter (Table 4). Sponge borings (Entobia) dominate the ichnocoenosis (Fig. 8A, 8B, Table 5). The thin covers of living coralline algae include plants of Lithothamnion, Lithophyllum, Harveylithon, and Sporolithon. Although the identification of coralline algal species in rhodolith interiors is difficult due to bioerosion, assemblages seem to be reduced to thin crusts of the melobesioid ‘‘morphotype 1’’ and Lithophyllum species (Fig. 8B, Table 6), with rare other components such as Sporolithon sp., Harveylithon sp., and Pneophyllum sp. Coral fragments are affected by microborings. Submarine cement fills the intraskeletal voids of corals, bryozoans, and coralline algae conceptacles

Deep Abrolhos Continental Shelf (50–75 m)

The rhodolith size ranges from ~ 1 to ~ 17 cm (Fig. 3, Table 2). Although spheroidal to subspheroidal shapes are the most common, subdiscoidal to discoidal rhodoliths account for 38% of the nodules measured (Table 2). As in the shallower ACS nodules, thin encrusting coralline algae partially or totally cover a structureless mass resulting from repeated phases of boring and filling the original framework of encrusting organisms (Fig. 7E, 7F). More than 70% of the rhodolith volume consists of a wackestone to packstone matrix, part of which fills well-defined borings (Fig. 8D–8F). At least three to four phases of boring and three

TABLE 3.—Mean and standard deviation (sd) of size (average of three measured axes) and significance level of size differences in rhodoliths from the study zones.

Size	Shallow SES	Deep SES	Shallow ACS	Deep ACS
Shallow SES n ¼ 77	mean ¼ 4.7 cm s.d. ¼ 1.2	p ,, 0.01 mean ¼ 7.8 cm	p ,, 0.01	p ,, 0.01

Deep SES		Not significant	Not significant
n ¼ 23	s.d. ¼ 3.1		
Shallow ACS		mean ¼ 7.2 cm	Not significant
n ¼ 192		s.d. ¼ 3.2	
Deep ACS			mean ¼ 6.6 cm
n ¼ 213			s.d. ¼ 3.3

phases of infilling can be distinguished. Entobia is the main ichnogenus with subordinate Gastrochaenolites and Trypanites (Fig. 8E, 8F, Table 5). The infilling sediment contains abundant spicules of ascidians and sponges, as well as articulated coralline algae, foraminifers, and bivalve fragments (Fig. 8F). Due to their internal structure the deeper ACS rhodoliths are denser than the ones from other areas. Siliciclastic grains comprise less than 2% of the nodules on average (Table 4). Living corallines at the surface comprise thin plants of unidentified melobesioids and Lithophyllum. Coralline assemblages inside the rhodoliths consist only of thin crusts, difficult to identify due to bioerosion. They include the melobesioid ''morphotype 1'', Lithophyllum species, Lithoporella, and rare Pneophyllum sp., laminar Mesophyllum, and Sporolithon (Table 6).

MDS Analysis

According to the proportions of different components, empty spaces, and trace fossils with and without filling, the rhodolith samples group into two main sets at a 60% similarity level. One comprises samples from shallow and deeper zones of SES and the other consists of the shallow and deep ACS rhodoliths (Fig. 9). The relative proportion of CCA, the extent of bioperforation with and without later infilling, and the amount of sediment/matrix are the main factors controlling the separation in two distinct groups (Table 5). Within the ACS samples the proportion of preserved CCA and the relative proportion of well-defined borings and sediment/matrix influence a certain segregation of deep from shallow rhodoliths.

Radiocarbon Dating

The CCA dated in the inner parts of deep SES rhodoliths yield ages of several hundred years cal BP, whereas near the surface they are younger than 250 years (Fig. 5J, 5K, Table 7). The measured inner part of a shallow ACS rhodolith has an age of 640 630 cal BP (Fig. 7G, Table 7). By contrast, dated structureless mass in the inner parts of the deeper ACS rhodoliths are thousands of years old (Fig. 7H, 7I, Table 7), whereas CCA near the surface

TABLE 4.—Percentage of calcium carbonate, organic matter and siliciclastic grains in rhodoliths from South of Esp´ırito Santo (SES) and Abrolhos Continental Shelf (ACS). Mean (6 standard deviation).

Region and depth	% $CaCo_3$	% Organic matter	% Siliciclastic grains
SES 20 m	90.02 (61.80)	4.55 (61.30)	5.43 (61.01)
SES 50 m	87.61 (62.90)	4.52 (61.39)	7.87 (62.62)
ACS 20 m	95.65 (60.85)	2.75 (61.24)	1.60 (61.31)
ACS 55 m	93.51 (61.45)	5.30 (61.36)	1.20 (60.11)
ACS 65 m	91.54 (61.36)	6.95 (61.36)	1.52 (60.19)

TABLE 5.—Percentage in rhodoliths of builders, trace fossils (with and without infilling sediments), voids, and matrix/sediment.

Rhodolith components (%)	SES (10–20 m)	SES (50–60 m)	ACS (20–30 m)	ACS (50–75 m)
Bryozoans	11.3	20.3	3.5	2.4
Corals	8.3	-	0.9	1.7
Crustose coralline algae	54.4	35.5	26.4	14.5
Foraminifera (total)	2.4	4.0	7.8	2.0
Arenaceous encrusting foraminifera	-	1.6	1.6	0.2
Calcareous encrusting foraminefera	2.1	1.0	4.0	0.6
Homotrema rubra (Lamarck 1816)	0.3	1.5	2.3	0.9
Peyssonneliaceans	1.4	2.5	2.0	1.0
Serpulids	1.2	2.0	2.4	1.0
Empty spaces/ voids	9.4	17.8	4.0	2.4
Macroborings (total)	1.7	1.5	50.0	33.0
Entobia	0.9	1.5	48.3	30.0
Gastrochaenolites	0.5	-	0.4	3.0
Trypanites	0.3	-	1.7	0.4
Matrix/sediments	8.6	20.2	1.9	41.5

(Fig. 7I) yield an age of a few hundred years period. In the oldest nodule collected at 75 m (Fig. 7I), there is a wide gap between the age of the inner and intermediate parts (about 7,300 and 6,000 years, respectively) and the age of its outer cover, indicating a long lasting interruption of its growth also shown by a marked change in color (Fig. 7I, Table 7).

TABLE 6.—Calcareous algal taxa in the interior of rhodoliths from South of Esp´ırito Santo (SES) and Abrolhos Continental Shelf (ACS) depths.

	SES		ACS	
Taxa	(10–20 m)	(50–60 m)	(20–30 m)	(50–75 m)
Harveylithon sp. (conceptacle 100 lm)	-	-	þ	-
Pneophyllum sp.	-	-	þ	þ
Spongites sp.	þ	-	-	-
Lithoporella sp.	-	-	þþ	þ
Lithophyllum gr. corallinae (Crouan and Crouan) Heydrich	þþ	þ	-	-
Lithophyllum prototypum (Foslie) Foslie	þ	þ	þþ	þþ
Lithophyllum gr. pustulatum (Lamouroux) Foslie	þ	þ	þþ	þþ
Lithothamnion crispatum Hauck	þþþ	þ	-	-
Lithothamnion muelleri Lenormand ex Rosanoff	þ	þþþ	-	-
Mesophyllum cf. engelhartii (Foslie) Adey	-	-	-	þ
Melyvonnea erubescens (Foslie) Athanasiadis and Ballantine	þþ	-	-	-
Morphotype 1 (thin thallus with plumose hypothallus)	-	þ	þþ	þþ
Sporolithon spp.	þ	þþ	þ	þ
Total CCA (13)	8	6	7	7
Peyssonnelia spp.	þ	þ	þ	þ

DISCUSSION

Rhodolith characteristics are influenced by the environmental conditions in which they grow, their ecological interactions and their age (Steller and Foster 1995; Marrack 1999; Foster 2001). The study SES and ACS areas differ in continental shelf geomorphology and width (Bastos et al. 2015), the degree of freshwater influx, coastal habitats, sedimentation patterns and biological aspects (Knoppers et al. 1999). Consequently, although they have some characteristics in common, rhodoliths from these two areas differ in several key features, such as inner arrangement, species composition, proportion of empty spaces and degree of bioerosion.

Rhodolith Size and Shape

The poor sorting of rhodolith size in the two ACS zones and deep SES rules out any marked influence of hydrodynamic forcing in rhodolith concentrations (Fig. 3). The small rhodoliths from shallow SES differ significantly in size from the rest (Table 3). The lack of marked sorting within the small and intermediate size ranges (Fig. 3) suggests that absence of rhodolith sizes over 8 cm is due to death/stop of nodule growth caused by burial rather than to hydrodynamic selection.

Spheroidal to subspheroidal rhodoliths predominate in ACS and SES areas as well as in other rhodolith beds along the Brazilian coast (Amado-Filho et al. 2007; Bahia et al. 2010; Pascelli et al. 2013). The predominance of spheroidal and subspheroidal shapes may be due to the frequent overturning of rhodoliths caused by water motion (Bosellini and Ginsburg 1971) as well as by the activity of various benthic organisms such as echinoderms, crustaceans, fish, and boring species (Prager and Ginsburg 1989; Marrack 1999; Pereira-Filho et al. 2015). The occurrence of discoidal to subdiscoidal shapes increases with depth, most markedly in ACS. Ellipsoidal rhodolith shapes show a slight decrease with depth in both regions. The higher abundance of discoidal nodule shapes was interpreted by Amado-Filho et al. (2007) as the result of less frequent overturning due to lower turbulence with increasing depth. This pattern was observed by Checconi et al. (2010), in middle-Miocene deposits from Vitulano (Southern Apennines, Italy), where rhodoliths from shallower and high-energy conditions were subspheroidal in shape and rhodoliths from deeper and less turbulent habitats were discoidal and ellipsoidal in shape. However, other studies show little or no correlation between shape, depth,

TABLE 7.—Calibrated radiocarbon ages of different parts of rhodoliths from South of Esp´ırito Santo (SES) and Abrolhos Continental Shelf (ACS) depths. See Figures 5J, 5K and 7G, 7H for location of dated areas in each rhodolith.

Area and depth	Rhodolith part/drilled component	Age (years cal BP)
SES (50 m)	Innermost/coralline algae	470–330
	Intermediate/coralline algae	490–410
	Surface/coralline algae	, 250
SES (50 m)	Inner/coralline algae	660–560
ACS (20 m)	Inner/structureless mass	610–670

ACS (65 m)	Innermost/structureless mass	2340–2150
ACS (75 m)	Innermost/structureless mass	7360–7210
	Intermediate/structureless mass	6010–5900
	Surface/coralline algae	330–260

and water movement (Reid and MacIntyre 1988; Prager and Ginsburg 1989; Steller and Foster 1995; Bassi et al. 2009; Braga 2017). In contrast to modern rhodoliths in other regions and fossil examples, in which the size and shape of nuclei determine the size and shape of rhodoliths (Bosence and Pedley 1982; Braga and Mart´ın 1988; Gischler and Pisera 1999; Lund et al. 2000; Vale et al. 2018), in the study areas the nuclei, if identifiable, are small and did not control the subsequent nodule growth.

Siliciclastic Content and Residence Time

Rhodoliths from SES show higher amounts of siliciclastic components than the ones from ACS. Remarkably, deep SES rhodoliths from 50–60 m have five- to 6.5-fold more siliciclastics than rhodoliths from similar depths in ACS. In SES the Brazilian continental shelf is narrower (Fig. 1), and therefore closer to the continent. The Itapemirim and Itabapoana rivers supply siliciclastics, increasing the water turbidity (Albino et al. 2006). By contrast, the sampling sites in the central ACS are distant from the shoreline (Fig. 1) and less subjected to siliciclastic sedimentation (Segal and Castro 2011). In general, in the ACS the discharge of fresh water is inversely correlated with the proportion of carbonate sediment (Knoppers et al. 1999), which increases from the region nearest the shoreline (50%) to the outer shelf (90%; Melo et al. 1975; Bastos et al. 2015). Carbonate sand and gravels are the typical sediments of the mid- and outer ACS (Milliman and Amaral 1974; Melo et al. 1975) and can cover up to 40% of the rhodolith-bed surface area (Brasileiro et al. 2015) (Fig. 1). Coral reefs are less abundant in the inner shelf (~ 10 km offshore) than in the mid- and outer ACS due to the greater influx of terrigenous sediment.

The higher terrigenous influx and seabed mobility might be the cause of the smaller mean diameter and size range of rhodoliths from the proximal SES area. Fine-grained siliciclastic sediment hinders rhodolith growth (Milliman 1977; Figueiredo et al. 2009) and probably limits rhodolith size before burial, also promoted by seabed mobility. Higher sediment influx could also be the reason for generally younger ages of SES rhodoliths compared to those from ACS, as the residence time on the sea floor for rhodoliths to grow is probably reduced by higher sedimentation rates.

Internal Structure

The internal structure is the main feature underlying the strong distinction of rhodoliths from the two regions shown by the MDS analysis. Most SES rhodoliths (85.7%) show a laminar, concentric to boxwork interior, with large amounts of constructional voids, either empty or filled by muddy sediment. There is a substantial increase in the proportion of constructional voids with depth in the SES rhodoliths. Although the presence of protuberant growth forms can partly account for void formation (Nitsch et al. 2015), high percentages of constructional voids have been related to low hydrodynamic energy (Braga and Mart´ın 1988; Bassi et al. 2009). The higher amount of voids in the deeper SES rhodoliths built by less protuberant corallines suggests that low turbulence is the main factor controlling the high constructional porosity in nodules from the deep zone. By contrast, rhodoliths in ACS consist mainly of a structureless mass, which comprises most of the rhodolith interior, covered by poorly developed laminar external coralline crusts. The structureless mass results from dense multiphase bioerosion, which is the cause of the sharp differences in internal structure between rhodoliths from the two regions. Rhodoliths on fore reef slope at 50 m depth in Bermuda show similar internal structure attributed to repeated episodes of bioerosion and cementation (Focke and Gebelein 1978). The high productivity in the ACS region (Moura et al. 2013; Cavalcanti et al. 2013; Ghisolfi et al. 2015; Reis et al. 2016) together with long residence times on the sea floor (see below) appear to be the main factors controlling the dense bioerosion observed in these nodules. Long residence times are favored by reduced terrigenous sediment influx reaching the central ACS, far from the shoreline. In accordance with this, older nodules in ACS show a more compact and denser structureless mass than do younger ones. More rapid burial prevents strong destruction of the rhodolith framework by intense bioerosion in SES, where productivity is similar to that in ACS (Costa et al. 2014).

Coralline Algae, Other Encrusters and Bioeroders

Thin encrusting coralline algae (Lithophyllum species, the melobesioid morphotype 1, and Lithoporella sp.) are thought to be the main builders of ACS rhodoliths in both depth zones. They can be identified mainly in the outer cover, whereas interior taxa are not known. Rhodoliths from SES are formed by thicker encrusting and warty coralline algae, mainly Lithothamnion and Mesophyllum species. Lithothamnion in SES is represented by L. crispatum at 10–20 m and L. muelleri at 50–60 m.

There are 33 CCA morpho-species documented on rhodolith surfaces on the continental shelf, seamounts and oceanic islands of Brazil, most of which occur in tropical waters (Amado-Filho et al. 2017). By contrast, only 13 fossil taxa were identified in the interior of rhodoliths from ACS and SES (Table 6). Seven of these are morpho-species that have been recorded living on rhodolith surfaces (Amado-Filho et al. 2017). The fossil Harveylithon specimens in the shallow ACS have very small conceptacles and probably correspond to the living coralline reported as Hydrolithon rupestre by Amado-Filho et al. (2010), Bahia (2014), and Brasileiro et al. (2015). Corallines identified at the genus and subfamily level may also correspond to living members of those taxa on the Brazilian shelf. A Lithoporella species found in the interior of deep ACS rhodoliths has not been recorded in living assemblages.

From the 11 species of CCA reported on the rhodolith surfaces on the SES (Amado-Filho et al. 2010; Bahia 2014) only five species were identified in the rhodoliths studied from this region: Lithothamnion crispatum, Lithothamnion muelleri, Melyvonnea erubescens, Lithophyllum gr. corallinae, and Lithophyllum gr. pustulatum. Lithophyllum prototypum, also found in the rhodoliths, was recorded in the Vit´oria-Trindade Chain (ES state; Pereira-Filho et al. 2012; Bahia 2014).

Lithothamnion, a common builder in SES rhodoliths, is considered by Pascelli et al. (2013) as the most important rhodolith-forming genus in the southwestern Atlantic. It is the most abundant genus in rhodolith beds from the eastern (Amado-Filho et al. 2012a; Brasileiro et al. 2015), northeastern (Riul et al. 2009) and southern Brazilian shelf (Pascelli et al. 2013). Lithothamnion crispatum is the most abundant species of Lithothamnion in the tropical Brazilian shelf (Pascelli et al. 2013; Bahia 2014). This species is recorded from a wide range of depths and is thought to have a long stratigraphic range, from the early Miocene (~ 20 My ago) to Recent, without significant morphological changes (Coletti et al. 2016).

Only two species (Lithophyllum gr. pustulatum and L. prototypum) and five genera (Lithophyllum, Harveylithon, Pneophyllum, Mesophyllum, and Sporolithon) out of the 14 living species included in eight genera of crustose coralline reported by Brasileiro et al. (2015) have been identified in the ACS rhodoliths. The low number of taxa recognized in the rhodolith interiors is probably due to the intense bioerosion, which destroyed the original building thalli, making identification difficult at the morpho-species level.

Bryozoans are more significant components in SES rhodoliths than in ACS ones. In the former region their abundance clearly increases with depth. The abundance of foraminifers, especially Homotrema rubrum, peaks in shallow ACS rhodoliths, while corals fragments are more frequent in the ACS deeper zone, reflecting the higher frequency of coral reefs in the mid- and outer ACS shelf.

Entobia is the most abundant ichnogenus at both depths (~ 50%). The boring sponge Cliona producing this bioperforation (Muricy et al. 2011) is abundant in ACS reefs and rhodoliths beds (F. Moraes personal communication 2016). Santos (2017) reports five boring sponge species in the shallow reefs of ACS: Cliona carteri (the most frequent), C. delitrix, C. schmidtii, C. varians, and Siphonodictyon coralliphagum, the last three with low abundance (, 2%). The boring sponges are more abundant in the outer than in the inner reefs, where the amounts of terrigenous sediment are higher (Santos 2017). The Entobia, Gastrochaenolites, and Trypanites ichnocoenosis, common at both shallow and deeper zones in ACS, was believed to reflect very shallow water depth (Taylor and Wilson 2003). However, Bassi et al. (2011, 2012, 2013) document this ichnocoenosis from deep-water rhodoliths (down to 100 m depth) in the Pacific Ocean.

The rhodoliths dated in this study could be older than the ages measured (mainly those from ACS), as the ages determined can be affected by mixing of younger carbonate due to complex multiphase boring and infilling processes. Even if a selective drilling of the original CCA framework was attempted, the contamination by younger sediments could not be completely avoided. The oldest dated rhodolith is from ACS (75 m depth). In this particular case, a dark colored core (Fig. 7I) suggests it was buried in organic-matter-rich, anoxic sediments for a long period after having grown from about 7,000 to 6,000 years BP. In any case, the interpretation of the bioeroded interior of ACS rhodoliths as pre-Holocene relict nuclei can be discarded. Such hypothesis was proposed for some (not all) intensely bioeroded nuclei of deep-water Caribbean rhodoliths studied by Reid and MacIntyre (1988). Although only few radiocarbon datings are available in ACS, the ages of the structureless-mass interiors range from about 7,300 to 600 cal year BP. Any pre-Holocene relict nucleus on ACS at depths from 75 to 20 m had to have formed at least between about 40,000 and 80,000 years ago (see sea level curves by Rohling et al. 2014) and their C^{14} content would be exhausted, making impossible radiocarbon Holocene ages such as the ones obtained, even if boring infillings introduced young carbonate. The structureless interiors cannot be fragments from in situ build ups. Samples were collected from separate sites in rhodoliths beds consisting of millions of rhodoliths, spread over hundreds of square kilometers both at the surface and at the top decimeters of the sediment pile. All examined rhodoliths in Abrolhos shelf share the same structure (interior parts made of a structureless mass) and no algal build ups have been observed in any of the sites. ACS rhodoliths simply acted as carbonate hard substrates on the sea floor for long intervals and were affected by multiphase bioerosion that destroyed their original frameworks.

CONCLUSIONS

Rhodoliths from SES consist of red algal crusts, subordinated bryozoans with concentric to boxwork inner arrangement and high porosity. Sediment infill of borings and voids includes a high amount of siliciclastics. Lithothamnion species and other melobesioids are the most common coralline algae. Rhodoliths from ACS are made of a structureless carbonate mass with thin encrusting coralline algae on the surface. The carbonate mass is produced by several phases of intense boring and infilling by wackestone to packstone, with low amounts of siliciclastics. Coralline assemblages are reduced to thin crusts of a few genera, mainly melobesioids and Lithophyllum. Rhodoliths from ACS are generally older than SES rhodoliths.

The observed differences on the internal structure and composition of rhodoliths reflect dissimilar growth histories due to local environmental conditions (distance to shoreline and sediment influx). Although both regions have similar high nutrient levels, delayed burial in ACS favors long-lasting intense boring of rhodoliths. This information, still scarce for the Brazilian coast, could be fundamental for conservation initiatives related to marine biodiversity. At the same time, it can be used to interpret the paleoenvironmental context of development of fossil rhodolith beds common in the geological record.

ACKNOWLEDGMENTS

Financial support to the Rede Abrolhos Network group was provided by: PELD and Mudan¸cas Clima´ticas Scientific Programs of the Brazilian National Science Agency (CNPq), Brazilian IODP Program (CAPES/MEC), P&D Program ANP/Brasoil (48610.011015/2014-55) and Research grants from FAPERJ (GMAF and RLM) and CNPq (ACB, GMAF, RLM). PSB and RNL acknowledge post-doctoral fellowship grants from CAPES/MEC. JCB was funded by the Brazilian Science and Technology Ministry within the Program Science Without Borders, project MCTI/MEC no. 400654/2014-8 ‘‘Recons-tru¸ca˜o Paleoecol ogica´ e Paleoclima´tica da Plataforma Continental de Abrolhos’’ (Paleoecological and Paleoclimatic reconstruction of Abrolhos Continental Shelf). We are grateful to two anonymous reviewers whose comments greatly improved the former version of this article.

REFERENCES

Adey, W.H. and MacIntyre, I.G., 1973, Crustose coralline algae: a re-evaluation in the geological sciences: Geological Society of America Bulletin, v. 84, p. 883–904.

Aguirre, J., Braga, J.C., and Bassi, D., 2017, Rhodoliths and rhodolith beds in the rock record, in R. Riosmena-Rodr´ıguez, W. Nelson, and J. Aguirre (eds.), Rhodolith/M¨aerl Beds: A Global Perspective: Springer, Berlin Heidelberg, Coastal Research Library, v. 15, p. 105–138.

AGUIRRE, J., BRAGA, J.C., MARTÍN, J.M., AND BETZLER, C., 2012, Paleoenvironmental and stratigraphic significance of Pliocene rhodolith beds and coralline algal bioconstructions from the Carboneras Basin (SE Spain): Geodiversitas, v. 34, p. 115–136.

Albino, J., Girardi, G., and Nascimento, K.A., 2006, Erosa˜o e prograda¸ca˜o do litoral do Espirito Santo, in D. Muehe (ed.), Erosa˜o e prograda¸ca˜o do litoral do Brasil: Minist´erio do Meio Ambiente, Bras´ılia, p. 227–264.

Amado-Filho, G.M., Bahia, R.G., Pereira Filho, G.H., and Longo, L.L., 2017, South Atlantic rhodolith beds: latitudinal distribution, species composition, structure and ecosystem functions, threats and conservation status, in R. Riosmena-Rodr´ıguez, W. Nelson, and J. Aguirre (eds.), Rhodolith/Ma¨erl Beds: A Global Perspective: Springer, Berlin Heidelberg, Coastal Research Library, v. 15, p. 299–317.

Amado-Filho, G.M., Manevelt, G., Manso, R.C.C., Marins-Rosa, B.V., Pacheco, M.R., and Guimara˜es, S.M.P.B., 2007, Structure of rhodolith beds from 4 to 55 meters deep along the southern coast of Esp´irito Santo State, Brazil: Ciencia Marina, v. 33, p 1–12. Amado-Filho, G.M., Manevelt, G.W., Pereira-Filho, G.H., Manso, R.C.C., Bahia, R.G., BARROS-BARRETO, M.B., AND GUIMARAES, S.M.P.B., 2010, Seaweed diversity associated with a Brazilian tropical rhodolith bed: Ciencia Marina, v. 36, p. 371–391.

Amado-Filho, G.M., Moura, R.L., Bastos, A.C., Francini-Filho R.B., Pereira-Filho,

G.H., Bahia, R.G., Moraes, F.C., and Motta, F.S., 2016, Mesophotic ecosystems of the unique South Atlantic atoll are composed by rhodolith beds and scattered consolidated reefs: Marine Biodiversity, v. 43, p. 933–936.

Amado-Filho, G.M., Moura, R.L., Bastos, A.C., Salgado, L.T., Sumida, P.Y., Guth, A.Z.,

Francini-Filho, R.B., Pereira-Filho, G.H., Abrantes, D.P., Brasileiro, P.S., Bahia, R.G., Leal, R.N., Kaufman, L., Kleypas, J.A., Farina, M., and Thompson, F.L., 2012a, Rhodolith beds are major $CaCO_3$ bio-factories in the tropical south west Atlantic: PloS One, v. 7, p. e35171.

Amado-Filho, G.M., Pereira-Filho, G.H., Bahia, R.G., Abrantes, D.P., Veras, C.P., and Matheus, Z., 2012b, Occurrence and distribution of rhodolith beds on the Fernando de Noronha Archipelago of Brazil: Aquatic Botany, v. 101, p. 41–45.

Bahia, R.G., 2014, Algas coralina´ceas formadoras de rodolitos da plataforma continental tropical e ilhas oceˆanicas do Brasil: inventa´rio flor´ıstico e taxonom´ıa: Unpublished Ph.D. Thesis, Instituto de Pesquisas Jardim Botˆanico do Rio de Janeiro, Rio de Janeiro, 220 p.

Bahia, R.G., Abrantes, D.P., Brasileiro, P.S., Pereira Filho, G.H., and Amado-Filho,

G.M., 2010, Rhodolith bed structure along a depth gradient on the northern coast of Bahia State, Brazil: Brazilian Journal of Oceanography, v. 58, p. 323–337.

Bassi, D., Humblet, M., and Iryu, Y., 2011, Recent ichnocoenosis in deep water macroids, Ryukyu Islands, Japan: PALAIOS, v. 26, p. 232–238.

Bassi, D., Iryu, Y., Braga, J.C., Takayanagi, H., and Tsuji, T., 2013, Bathymetric distribution of ichnocoenoses from Recent subtropical algal nodules off Fraser Island, eastern Australia: Palaeogeography. Palaeoecology, Palaeoclimatology, v. 369, p. 58–66. Bassi, D., Iryu, Y., Humblet, M., Matsuda, H., Machiyama, H., Sasaki, K., Matsuda, S.,

Arai, K., and Inoue, T., 2012, Recent macroids on the Kikai-jima shelf, Central Ryukyu Islands, Japan: Sedimentology, v. 59, p. 2024–2041.

Bassi, D., Nebelsick, J.H., Checconi, A. Hohenegger, J., and Iryu, Y., 2009, Present-day and fossil rhodolith pavements compared: their potential for analyzing shallow-water carbonate deposits: Sedimentary Geology, v. 214, p. 74–84.

Bastos, A.C., Quaresma, V.S., Marangoni, M.B., D'Agostini, D.P., Bourguignon, S.N., Cetto, P.H., Silva, A.E., Amado-Filho, G.M., Moura, R.L., and Collins, M., 2015, Shelf morphology as an indicator of sedimentary regimes: a synthesis from a mixed siliciclastic-carbonate shelf on the eastern Brazilian margin: Journal of South American Earth Science, v. 63, p. 125–136.

Bosence, D.W.J., 1983a, The occurrence and ecology of recent rhodoliths—a review, in T.M. Peryt (ed.), Coated Grains: Springer-Verlag, Berlin Heidelberg, p. 225–242.

Bosence, D.W.J., 1983b, Coralline algal reef frameworks: Journal of the Geological Society, v. 140, p. 365–376.

Bosence, D.W.J., 1984, Construction and preservation of two modern coralline algal reefs, St. Croix, Caribbean: Palaeontology, v. 27, p. 549–574.

Bosence, D.W.J. and Pedley, H.M., 1982, Sedimentology and palaeoecology of a Miocene coralline algal biostrome from the Maltese Islands: Palaeogeography, Palaeoclimatology, Palaeoecology, v. 38, p. 9–43.

Bosselini, A. and Ginsburg, R.N., 1971, Form and internal structure of Recent algal nodule from Bermuda: Journal of Geology, v. 79, p. 669–682.

Braga, J.C., 2017, Neogene rhodoliths in the Mediterranean basis, in R. Riosmena-Rodr´ıguez, W. Nelson, and J. Aguirre (eds.), Rhodolith/Ma¨erl Beds: A Global Perspective: Springer, Berlin Heidelberg, Coastal Research Library 15, p.169–193.

Braga, J.C. and Aguirre, J., 2001, Coralline algal assemblages in upper Neogene reef and temperate carbonates in Southern Spain: Palaeogeography, Palaeoclimatology, Palaeo-ecology, v. 175, p. 27–41.

Braga, J.C., Bassi, D., and Piller, W.E., 2010, Palaeoenvironmental significance of Oligocene–Miocene coralline red algae—a review, in M. Mutti, W.E. Piller, and C. Betzler (eds.), Carbonate Systems During the Oligocene–Miocene Climatic Transition: IAS Special Publications, v. 42, p. 165–182.

Braga, J.C., Martín, J.M., 1988, Neogene coralline-algal growth-forms and their palaeoenvironments in the Almanzora River Valley (Almeria, SE Spain): Palaeo-geography, Palaeoclimatology, Palaeoecology, v. 67, p. 285–303.

Brandano, M., Tomassetti, L., Bosellini, F., and Mazzuchi, A., 2010, Depositional model and paleodepth reconstruction of a coral-rich, mixed siliciclastic–carbonate system: the Burdigalian of Capo Testa (northern Sardinia, Italy): Facies, v. 56, p. 433–444.

Brasileiro, P.S., Pereira-Filho, G.H., Bahia, R.G., Abrantes, D.P., Guimaraes˜, S.M.P.B., and Moura, R.L., 2015, Macroalgal composition and community structure of the largest rhodolith beds in the world: Marine Biodiversity, v. 46, p. 407–420.

Bruce, T., Meirelles, P.M., Garcia, G., Paranhos, R., Rezende, C.E., Moura, R.L., Coni, E.O.C., Vasconcelos, A.T., Amado Filho, G.M., Hatay, M., Schmieder, R., Edwards, R., Dinsdale, E., Thompson, F.L., 2012, Abrolhos bank reef health evaluated by means of water quality, microbial diversity, benthic cover, and fish biomass data: PloS One, v. 7,
e36687.

Cavalcanti, G.S., Gregoracci, G.B., Longo, L.L., Bastos, A.C., Ferreira, C.M., Francini-Filho, R.B., Pereira-Filho, G.H., Abrantes, D.P., Guimaraes, S.M.P.B., Moura, R.L., Amado-Filho, G.M., Hatay, M., Schmieder, R., Edwards, R.D., Dinsdale, E.A., Thompson, F.L., 2013, Sinkhole-like structures as bioproductivity hotspots in the Abrolhos Bank: Continental Shelf Research, v. 70, p. 126–134.

Checconi, A., Bassi, D., Carannante, G., and Monaco, P., 2010, Re-deposited rhodoliths in the middle Miocene hemipelagic deposits of Vitulano (Southern Apennines, Italy): coralline assemblage characterization and related trace fossils: Sedimentary Geology, v. 225, p. 50–66.

Clarke, R.K. and Warwick, R.M., 1994, Change in marine communities: an approach to
statistical analysis and interpretation (Plymouth (UK): Natural Environment Research
Council-Plymouth Marine Laboratory, Plymouth, ISBN-13: 978-1855311404, 144 p.

Coletti, G., Rabovsky´, J., and Basso, D., 2016, Lithothamnion crispatum: long-lasting species of non-geniculate coralline algae (Rhodophyta, Hapalidiales): Carnets de G´eologie, v. 16, p. 27–41.

Costa, E.S., Andrade, R.R., Junior, L.B., Gaigher, L.P., Oliveira, C.M.S., Junior, C.D., and Neto, R.R., 2014, Controls on temporal and spatial variation of nutrients in a tropical marine artificial reef: the case of the Victory 8B on the southeastern Brazilian Coast: Revista Virtual de Qu´ımica, v. 6, p. 834–843.

Figueiredo, A.G., Silva, F.T., Pacheco, C.E.P., Vasconcelos, S.C., and Kowsmann,

R.O., 2009, Sedimentologia da plataforma continental da Bacia de Campos: 138 Congress of The South America Quaternary, Challenges and Perspectives, Arma¸ca˜o dos Buzios,´ 5 p.

Focke, J.W. and Gebelein, C.D., 1978, Marine lithification of reef rock and rhodolites at a fore-reef slope locality (50m) off Bermuda: Geologie en Mijnbouw, v. 57, p. 163–171 Foster, M.S., 2001, Rhodoliths: between rocks and soft places—Minireview: Journal of
Phycology, v. 37, p. 659–667.

Ginsburg, R.N. and Schroeder, J.H., 1973, Growth and submarine fossilization of algal cup reefs, Bermuda: Sedimentology, v. 20, p. 575–614.

Gischler, E. and Pisera, A., 1999, Shallow water rhodoliths from Belize reef: Neues Jahrbuch fur¨ Geologie und Pal¨aontologie, v. 214, p. 71–93.

Ghisolfi, R.D., Silva, M.P., Santos, F.T., Servino, R.N., and Thompson, F.L., 2015, Physical forcing mechanisms controlling the variability of chlorophyll-a over the Royal-Charlotte and Abrolhos Banks-Eastern Brazilian Shelf: PLoS One, v. 10, e0117082.

Jones, C.G., Lawton, J.H., and Shachak, M., 1997, Positive and negative effects of organisms as physical ecosystem engineers: Ecology, v. 78, p. 1946–1957.

Kamenos, N.A., Heidi, L.B., and Darrenougue, N., 2017, Coralline algae as recorders of past climatic and environmental conditions, in R. Riosmena-Rodr´ıguez, W. Nelson, and J. Aguirre (eds.), Rhodolith/Ma¨erl Beds: A Global Perspective: Springer, Berlin Heidelberg, Coastal Research Library, v. 15, p. 27–53.

Knoppers, B.A., Bidone, E.D., and Abra˜o, J.J., 1999, Environmental geochemistry of coastal lagoon systems of Rio de Janeiro. Repport Geoqu´ımica Ambiental. Niter oi:´ Programa de Geoqu´ımica, Universidade Federal Fluminense, Financiadora de Estudos e Projetos, 210 p.

Leal, R.N., Bassi, D., Posenato, R., and Amado-Filho, G.M., 2012, Tomographic analysis for bioerosion signatures in shallow-water rhodoliths from the Abrolhos Bank, Brazil: Journal of Coastal Research, v. 28, p. 306–309.

Lund, M., Davies, P.J., and Braga, J.C., 2000, Coralline algal nodules off Fraser Island, Eastern Australia: Facies, v. 42, p. 25–34.

Marins, B.V., Amado-Filho, G.M., Barbarino, E., Pereira-Filho, G.H., and Longo, L.L.,

2014, Seasonal changes in population structure of the tropical deep-water kelp Laminaria abyssalis: Phycological Research, v. 62, p. 55–62.

Marrack, E.C., 1999, The relationship between water motion and living rhodolith beds in the southwestern Gulf of California, Mexico: PALAIOS, v. 14, p. 159–171.

Melo, U., Summerhayes, C., and Ellis, J.P., 1975, Part IV: Salvador to Vitoria, Southeastern Brazil, in J.D. Milliman and P.S. Colin (eds.), Upper Continental Margin Sedimentation off Brazil: Contributions to Sedimentology, v. 4, p. 78–116.

Milliman, J.D., 1977, Relict magnesian calcite oolite and subsidence of the Amaon shelf:
reply: Sedimentology, v. 24, p. 149–151.

Milliman, J.D. and Amaral, C.A.B., 1974, Economic potential of Brazilian continental margin sediments: Congresso Brasileiro de Geologia, v. 28, p. 335–344.

Moura, R.M., Secchin, N.A., Amado-Filho, G.M., Francini-Filho, R.B., Freitas, M.O., Minte-Vera, C.V., Teixeira, J.B., Thompson, F.L., Dutra, G.F., Sumida, P.Y.G., Guth, A.Z., Lopes, R.M., and Bastos, A.C., 2013, Spatial patterns of benthic megahabitats and conservation planning in the Abrolhos Bank: Continental Shelf Research, v. 70, p. 109– 117.

Muricy, G., Lopes, D.A., Hajdu, E., Carvalho, M., Moraes, F., Klautau, M., Menegola,

C., and Pinheiro, U.S., 2011, Catalogue of Brazilian Porifera: Rio de Janeiro, Museu Nacional, S´erie Livros, v. 46, 300 p.

Nebelsick, J.H. and Bassi, D., 2000, Diversity, growth-forms and taphonomy: key factors controlling the fabric of coralline algal dominated shelf carbonates, in E. Insalaco, P.W. Skelton, and T.J. Palmer (eds.), Carbonate Platform Systems: Components and Interactions: Geological Society Special Publications, v. 178, p. 89–107.

Nitsch, F., Nebelsick, J.H., and Bassi, D., 2015, Constructional and destructional patterns—void classification of rhodoliths from Giglio Island, Italy: PALAIOS, v. 30, p. 680–691.

Oliveira, K.S.S. and Quaresma, V.S., 2017, Temporal variability in the suspended sediment load and streamflow of the Doce River: Journal of South American Earth Sciences, v. 78, p. 101–115.

Paloczy, A., Brink, K.H., Silveria, I.C., Arruda, W.Z., and Martins, R.P., 2016, Pathways and mechanisms of offshore water intrusions on the Esp´irito Santo Basin shelf (188S– 228S, Brazil): Journal of Geophysical Research, v. 121, p. 5134–5163

Pascelli, C., Riul, P., Riosmena-Rodriguez, R., Scherner, F., Nunes, M., Hall-Spencer,

J.M., Oliveira, E.C., and Horta, P., 2013, Seasonal and depth-driven changes in rhodolith bed structure and associated macroalgae off Arvoredo Island (southeastern Brazil): Aquatic Botany, v. 111, p. 62–65.

P EREIRA -F ILHO , G.H., A MADO -F ILHO , G.M., M OURA , R.L., B ASTOS , A.C., G UIMARAES ,

S.M.P.B., Salgado, L.T., Francini-Filho, R.B., Bahia, R.G., Abrantes, D.P., Guth, A.Z., and Brasileiro, P.S., 2012, Extensive rhodolith beds cover the summits of southwestern Altantic Ocean: Journal of Coastal Research, v. 28, p. 261–269.

Pereira-Filho, G.H., Veras, P.C., Francini-Filho, R.B., Moura, R.L., Pinheiro, H.T., Gibran, F.Z., Matheus, Z., Neves, L.M., and Amado-Filho, G.M., 2015, Effects of the sand tilefish Malacanthus plumieri on the structure and dynamics of a rhodolith bed in the Fernando de Noronha Archipelago, tropical West Atlantic: Marine Ecology Progress Series, v. 541, p. 65–73.

Prager, E.J. and Ginsburg, R.N., 1989, Carbonate nodule growth on Florida's outer shelf and its implications for fossil interpretations: PALAIOS, v. 4, p. 310–317.

Reid P.R. and MacIntyre, I.G., 1988, Foraminiferal-algal nodules from the eastern Caribbean: growth history and implications on the value of nodules as paleoenvironmental indicators: PALAIOS, v. 3, p. 424–435.

Reis, V.M., Karez, C.S., Mariath, R., Moraes, F.C., Carvalho, R.T., Brasileiro, P.S., Bahia, R.G., Lotufo, T.M.C., Ramalho, L.V., Moura, R.L., Francini-Filho, R.B., Pereira-Filho, G.H., Thompson, F.L., Bastos, A.C., Salgado, L.T., and Amado-Filho,

G.M., 2016, Carbonate production by benthic communities on shallow coralgal reefs of Abrolhos Bank, Brazil: PLoS ONE, v. 11, e0154417.

Riul, P., Lacouth, P., Pagliosa, P.R., Christoffersen, M.L., and Horta, P.A., 2009, Rhodolith beds at the easternmost extreme of South America: community structure of an endangered environment: Aquatic Botany, v. 90, p. 315–320.

Rohling, E.J., Foster, G.L., Grant, K.M., Marino, G., Roberts, A.P., Tamisiea, M.E., and Williams, F., 2014, Sea-level and deep-sea-temperature variability over the past 5.3 million years: Nature, v. 508, p. 477–482.

Santos, F.C., 2017, Avalia¸ca˜o espa¸co-temporal da composi¸ca˜o e abundˆancia das esponjas perfurantes nos recifes rasos do Banco dos Abrolhos, Bahia, Brasil: Unpublished MS Thesis, Instituto de Pesquisas Jardim Botˆanico do Rio de Janeiro, 67 p.

Segal, B. and Castro, C.B., 2011, Coral community structure and sedimentation at different distances from the coast of the Abrolhos Bank, Brazil: Brazilian Journal of Oceanography, v. 59, p. 119–129.

Sneed, E.D. and Folk, R.L., 1958, Pebbles in the Lower Colorado River, Texas: a study in
the particle morphogenesis: Journal of Geology, v. 66, p. 144–150.

Steller, D.L. and Foster, M.S., 1995, Environmental factors influencing distribution and morphology of rhodoliths in Bah´ıa Concepci on,´ B.C.S., M´exico: Journal of Experimental Marine Biology and Ecology, v. 194, p. 201–212.

T AMEGA , F.T.S., B ASSI , D., F IGUEIREDO , M.A.O., AND C HERKINSKY , A., 2014, Deep-water
rhodolith bed from central Brazilian continental shelf, Campos Basin: coralline algal and
faunal taxonomic composition: Galaxea, v. 16, p. 21–31.

Taylor, P.D. and Wilson, M.A., 2003, Paleoecology and evolution of marine hard substrate communities: Earth-Science Reviews, v. 62, p. 1–103.

Testa, V. and Bosence, D.W.J., 1999, Physical and biological controls on the formation of carbonate and siliciclastic bedforms on the north-east Brazilian shelf: Sedimentology, v. 46, p. 279–301.

Vale, N.V., Amado-Filho, G.M., Braga, J.C., Brasileiro, P.S., Karez, C.S., Moraes, F.C., Bahia, R.G., Bastos, A.C., and Moura, R.L., 2018, Structure and composition of rhodoliths from the Amazon River mouth, Brazil: Journal of South American Earth Sciences, v. 84, p. 149–159.

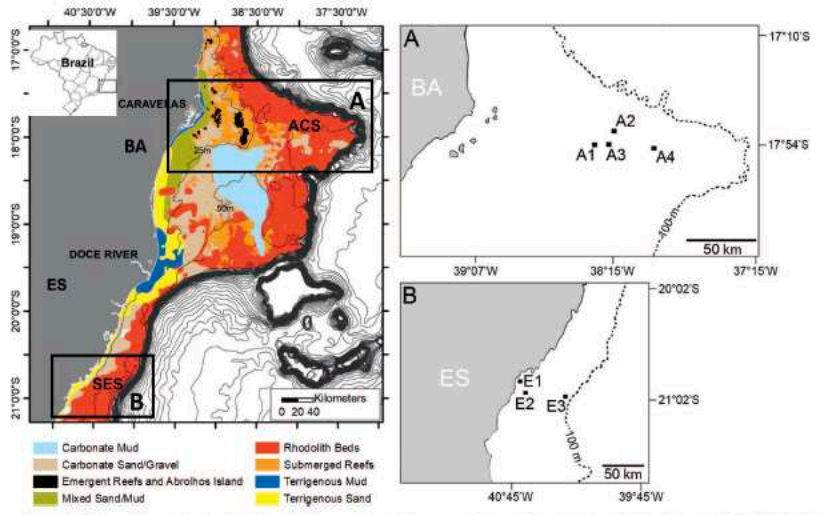

Fig. 1.—Studied area. Left, map showing distribution of sedimentary facies and the two sampled areas, ACS and SES (modified from Bastos et al. 2015). Right: A) Sampling sites on Abrolhos Continental Shelf; A1 and A2: 20–30 m; A3 and A4: 50–75 m. B) sampling sites on the continental shelf of the South Espirito Santo State; E1 and E2: 10–20 m; E3: 50–60 m. Abbreviations: ACS = Abrolhos Continental Shelf; SES = South Espirito Santo Shelf; ES = Espirito Santo; BA = Bahia.

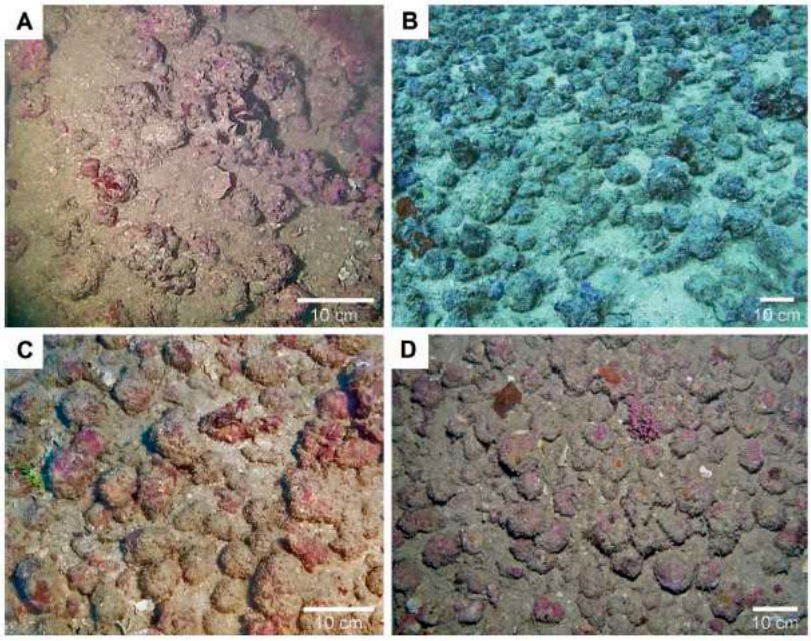

Fig. 2.—Rhodoliths beds. From South Espirito Santo: **A)** Shallow SES, 20 m depth. **B)** Deep SES, 50 m depth. From Abrolhos Continental Shelf: **C)** Shallow ACS, 30 m depth. **D)** Deep ACS, 55 m depth.

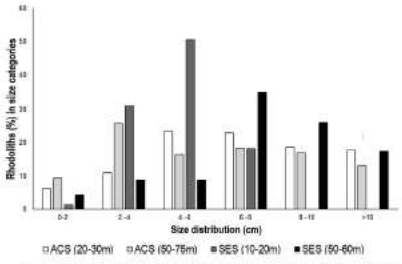

Fig. 3.—Size distribution of rhodoliths. Shallow SES zone (n = 77); deep SES (n = 23); shallow ACS (n = 192); deep ACS (n = 213). Note the absence of rhodoliths bigger than 8 cm at shallow SES.

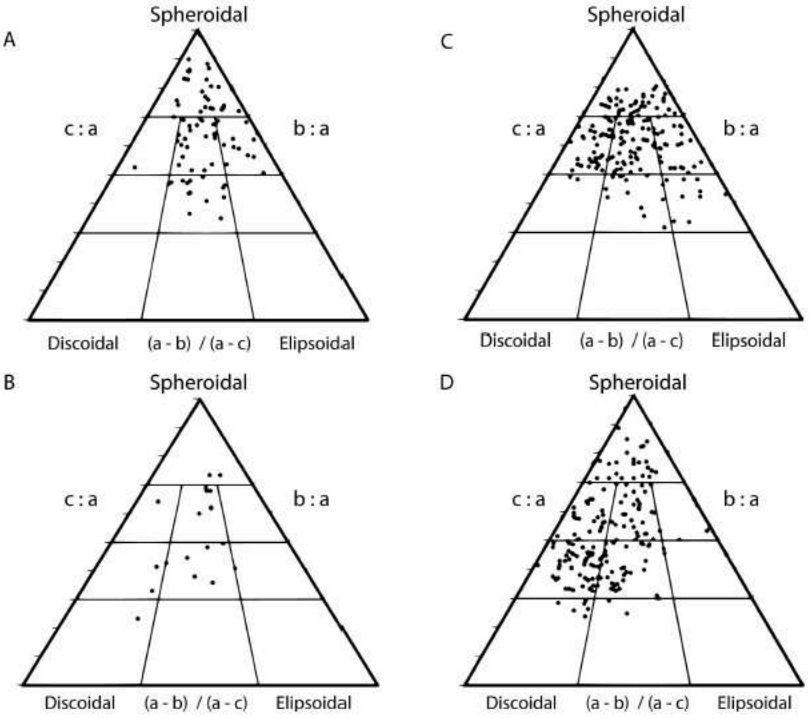

Fig. 4.—Rhodolith shape distribution using Sneed and Folk's (1958) sphericity diagram. Spheroidal and sub-spheroidal rhodoliths dominate the assemblages. **A)** Shallow SES zone (n = 77). **B)** Deep SES zone (n = 23). **C)** Shallow ACS zone (n = 192). **D)** Deep ACS zone (n = 213).

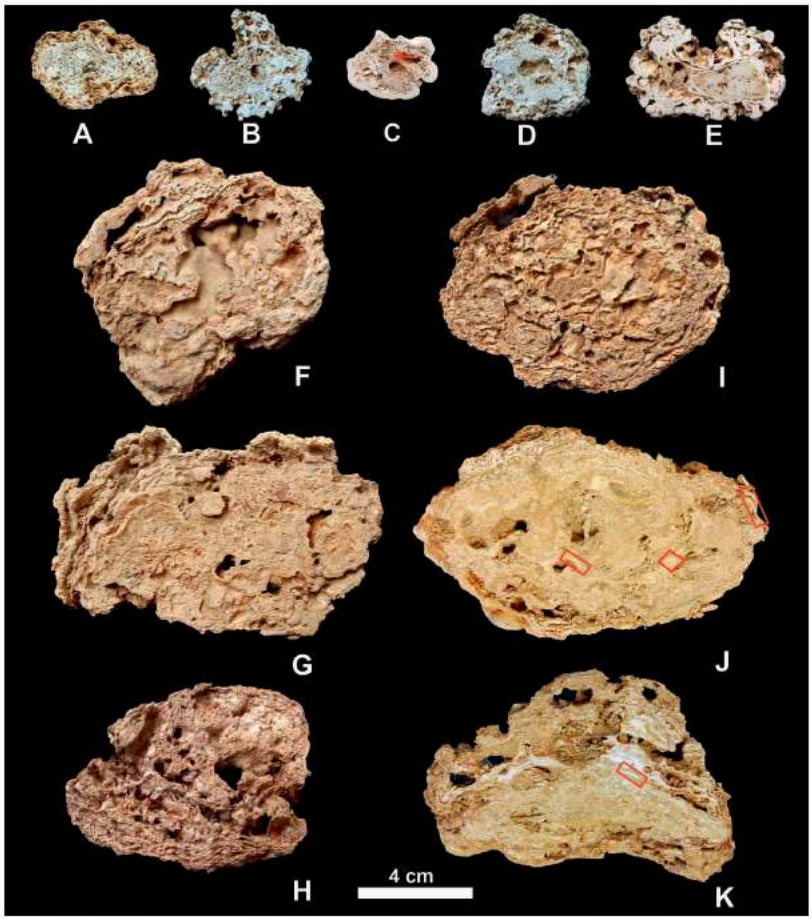

Fig. 5.—Rhodoliths from South Espirito Santo State (SES) showing laminar concentric and boxwork arrangement. Constructional voids can be observed between the laminar layers. Shallow SES (A–E): **A)** Sample ER1. **B)** Sample ER2. **C)** Sample ER3. Arrow points to partially dissolved coral skeleton. **D)** Sample ER4. **E)** Sample ER5. Deep SES (F–I): **F)** Sample EF1. **G)** Sample EF2. **H)** Sample EF3. **I)** Sample EF4. **J, K)** radiocarbon dated rhodoliths, deep SES. Red rectangles indicate location of dated CCA thalli.

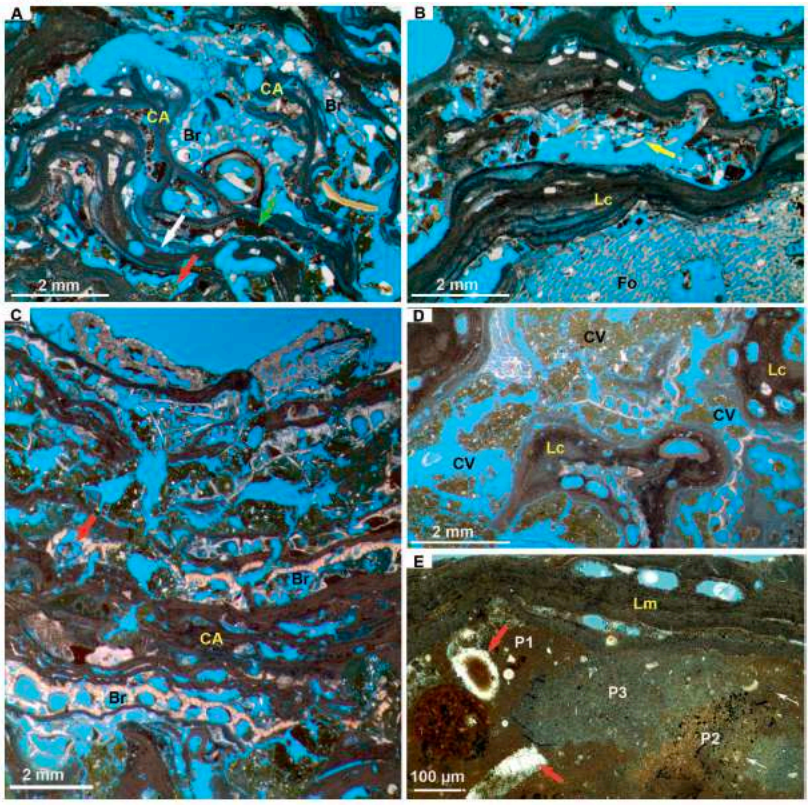

Fig. 6.—Micrographs of rhodoliths from South Espirito Santo State (SES). **A)** Shallow SES sample ER1, boundstone of crustose coralline algae (CA) intergrown with bryozoans (Br). White arrow points to a constructional void; green and red arrows point to a bioeroded first-phase and a second phase infillings, respectively. **B)** Shallow SES sample ER5, encrusting foraminiferal (Fo) fragment (nucleus) encrusted by *Lithothamnion crispatum* (Lc), the most frequent coralline species. Voids partially filled by grainstone rich in foraminifers (arrow). **C)** Deep SES sample EF4, boundstone of crustose coralline algae (CA) intergrown with bryozoans (Br) and encrusting foraminifers (arrow). **D)** Deep SES sample EF3, constructional voids (CV) originated by lumpy form of *Lithothamnion crispatum* (Lc), partially filled by sediment. **E)** Deep SES sample EF2, *Lithothamnion muelleri* (Lm), the most frequent coralline algal species at this depth. Multiphase infilling (P1–3) of constructional voids and borings by wackestone with siliciclastics (white arrows). Red arrows point to dissolved aragonite skeletons, which were dissolved and replaced with calcite.

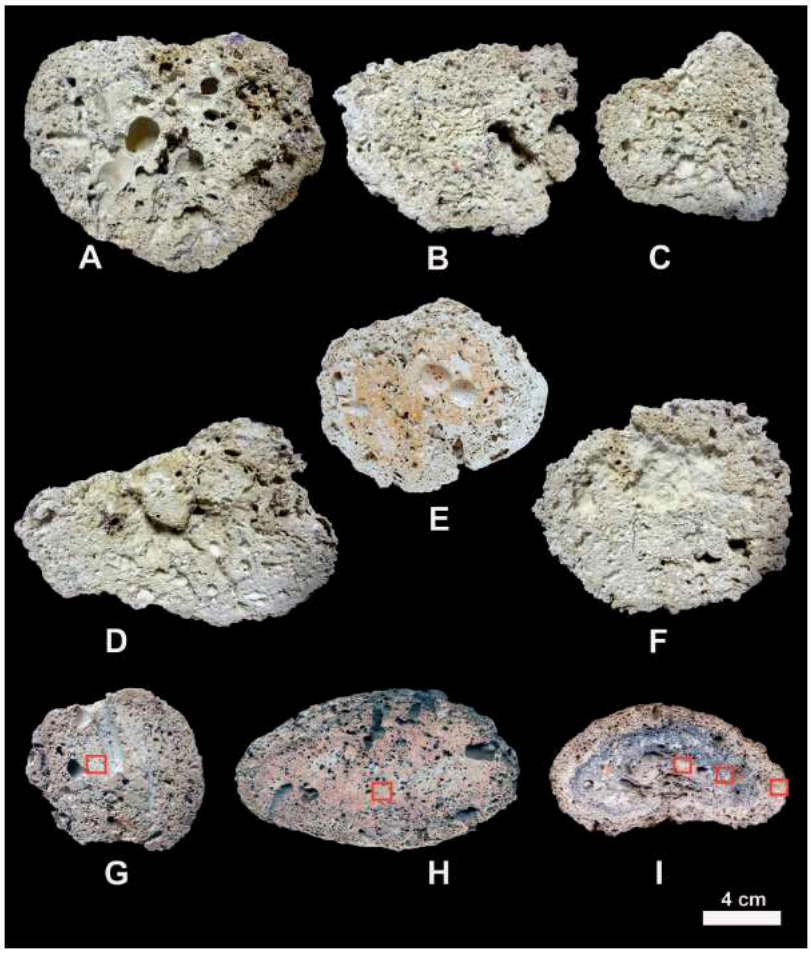

Fig. 7.—Rhodoliths from Abrolhos Continental Shelf (ACS) showing massive, structureless inner arrangement. A) Shallow ACS sample AB8. B) Shallow ACS sample AB7. C) Shallow ACS sample AB5. D) Shallow ACS sample AB6. E) Deep ACS sample AB4. F) Deep ACS sample AB3. G–I) Radiocarbon-dated rhodoliths. Red squares indicate location of dated areas: (G) shallow ACS, dated area is structureless mass; (H) deep ACS, 65 m, dated area from structureless mass; (I) deep ACS, 75 m, rhodolith with a dark colored core. Inner dated areas are structureless mass, whereas the outer corresponds to thin CCA cover.

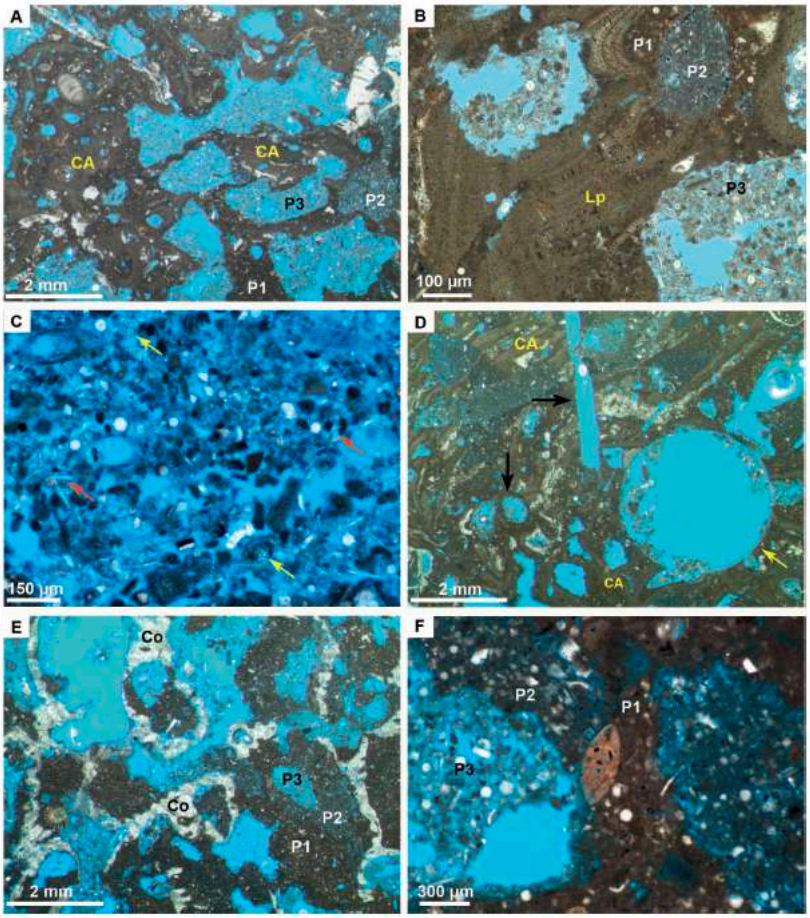

Fig. 8.—Micrographs of rhodoliths from Abrolhos Continental Shelf (ACS). Original coralline algal boundstones (CA) intensely bored with multiphase infilling (P1–3) by wackestones to packstones. A) Shallow ACS sample AB5, structureless carbonate mass (wackestone to packstone) produced by intense boring (*Entobia* predominantly) and infill. B) Shallow ACS sample AB7, bored *Lithophyllum* gr. *pustulatum* (Lp). Note 3 phases of boring (P1–3). C) Shallow ACS sample AB7, components of the third phase of infilling, mainly ascidian (yellow arrows) and sponge (red arrows) spicules. D) Deep ACS sample AB3, coralline algal boundstone (CA) intensively bored by *Entobia* (with multiphase infilling P1–3), *Gastrochaenolites* (yellow arrows) and *Trypanites* (black arrows). E) Deep ACS sample AB4, intensively bored coral fragment (Co). F) Deep ACS sample AB4, successive phases of filling (P1–3) wackestones to packstones. Note the large benthic foraminifer at the center of the image.

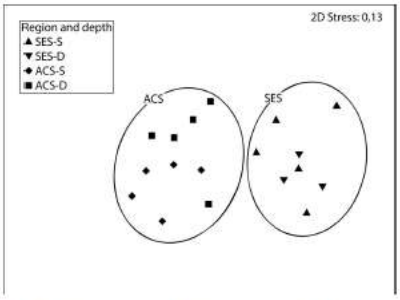

Fig. 9.—Multi-dimensional scaling (MDS) ordination based on proportions of organism groups, voids, borings (with and without infilling) and matrix/sediments (see Table 5) in rhodoliths of SES and ACS. Groups are circled at a 60% similarity level. SES-S and SES-D rhodoliths from shallow and deep SES zones, ACS-S and ACS-D rhodoliths from shallow and deep ACS zones, respectively.